

Review

# ‘What controls aqueous humour outflow resistance?’

Mark Johnson

*Department of Biomedical Engineering, Northwestern University, TECH E378, 2145 Sheridan Road, Evanston, IL 60208, USA*

Received 31 March 2005; accepted in revised form 7 October 2005

Available online 4 January 2006

## Abstract

The bulk of aqueous humour outflow resistance is generated in or near the inner wall endothelium of Schlemm’s canal in normal eyes, and probably also in glaucomatous eyes. Fluid flow through this region is controlled by the location of the giant vacuoles and pores found in cells of the endothelium of Schlemm’s canal, but the flow resistance itself is more likely generated either in the extracellular matrix of the juxtacanalicular connective tissue or the basement membrane of Schlemm’s canal. Future studies utilizing in vitro perfusion studies of inner wall endothelial cells may give insights into the process by which vacuoles and pores form in this unique endothelium and why inner wall pore density is greatly reduced in glaucoma.

© 2005 Elsevier Ltd. All rights reserved.

*Keywords:* glaucoma; Schlemm’s canal; hydraulic conductivity

It has been recognized for more than 130 years that the elevated pressure characteristic of primary open-angle glaucoma arises due to an increased resistance to the outflow of aqueous humour from the eye. (Leber, 1873) However, a conclusive determination of where in the outflow pathways this elevated outflow resistance is generated has been elusive. Surprisingly, the locus of aqueous humour outflow resistance in the normal eye has also been not been unequivocally determined.

Seidel (1921) using light microscopy, stated ‘that the inner wall of Schlemm’s canal stand in open communication with the anterior chamber, and that the aqueous humour directly washes around the inner wall endothelium of Schlemm’s canal and is only separated from the lumen of Schlemm’s canal by a thin, outer membrane’. Our view is little different today. The locus of outflow resistance, both in the normal eye and the glaucomatous eye, is thought to arise either in the endothelial lining of Schlemm’s canal, or very near to this location. In this article, current thoughts on where that flow resistance might be generated are reviewed.

There are a number of excellent review articles (Tripathi, 1974a,b; Bill, 1975; Bill and Mäepea, 1994; Gong et al., 1996; Johnson and Erickson, 2000; Ethier, 2002) that describe the detailed morphology and physiology of the aqueous outflow pathway. In this review, the evidence that leads to

the conclusion that the inner wall region is responsible for the bulk of aqueous humour outflow resistance is first presented. Then, attention is focused on those proximal aspects of this pathway that are nearest to the endothelial linings of Schlemm’s canal, and the transport characteristics of these structures.

The bulk of the aqueous humour flows out of the anterior chamber of the eye through the conventional aqueous outflow pathway comprised of the trabecular meshwork, the juxtacanalicular connective tissue, the endothelial lining of Schlemm’s canal, Schlemm’s canal itself, the collecting channels and aqueous veins, and then finally drains into the episcleral venous system, rejoining the blood from whence it came (in this review, the juxtacanalicular connective tissue is considered separately from the trabecular meshwork). A second ‘unconventional’ outflow pathways exists (Bill, 1964a,b, 1965; Bill and Helsing, 1965), but carries less than 10% of the total flow in the adult human eye, (Bill and Phillips, 1971) and thus does not significantly contribute to the dynamics of aqueous humour outflow in the normal eye. This pathway is important, however, to the understanding of the mechanism of action of PGF<sub>2α</sub> in the treatment of glaucoma. A review of transport through the unconventional outflow pathways can be found in Johnson and Erickson (2000).

## 1. Regions of low outflow resistance

In this section, those aspects of the conventional aqueous humour outflow pathway that are generally agreed to have

*E-mail address:* [mj-johnson2@northwestern.edu](mailto:mj-johnson2@northwestern.edu).

small or negligible outflow resistance are examined. These include the trabecular meshwork, Schlemm's canal and the collector channels and aqueous veins.

The uveal and corneoscleral meshworks, that make up the trabecular meshwork, are highly porous structures with numerous openings that range in size from 25–75  $\mu\text{m}$  in the proximal regions of the uveal meshwork to 2–15  $\mu\text{m}$  in the deeper layers of the corneoscleral meshwork (Tripathi, 1974a, b). McEwen (1958) used Poiseuille's law to show that a single pore 100  $\mu\text{m}$  long (the thickness of the trabecular meshwork in the flow-wise direction) and 20  $\mu\text{m}$  in diameter could carry the entire aqueous humour flow (2  $\mu\text{l}/\text{min}$ ) with a pressure drop of 5 mmHg, and thus concluded that there was negligible flow resistance in this region. Grant (1963) provided experimental support for this conclusion by cutting through the proximal aspects of the meshwork of enucleated human eyes and found no effect on outflow resistance.

Schlemm's canal, shown in Fig. 1, is the space that exists between the endothelial lining of the inner wall of Schlemm's canal, and the sclera. While the canal is open at low intraocular pressures, Johnstone and Grant (1973) showed that the trabecular meshwork expands and Schlemm's canal collapses as the intraocular pressure is increased. The distance between the inner and outer wall decreases from roughly 30  $\mu\text{m}$  for eyes fixed by immersion in fixative to a nearly zero when the eyes are fixed by perfusion with fixative at intraocular pressures (IOP) that exceeds episcleral venous pressure by approximately 30 mmHg. While the size of the canal at low IOP is much too large to generate a significant outflow resistance, (Moses, 1979) the collapse of Schlemm's canal at higher IOP has led some to speculate that this might be a cause of primary open-angle glaucoma. (Nesterov, 1970)

However, Johnson and Kamm (1983) pointed out that when outflow resistance is measured at high IOP in non-glaucomatous human eyes, the outflow resistance is not nearly as high as that of a glaucomatous eye. (Brubaker, 1975; Van Buskirk, 1976; Moses, 1977) Collapse of the canal would make a

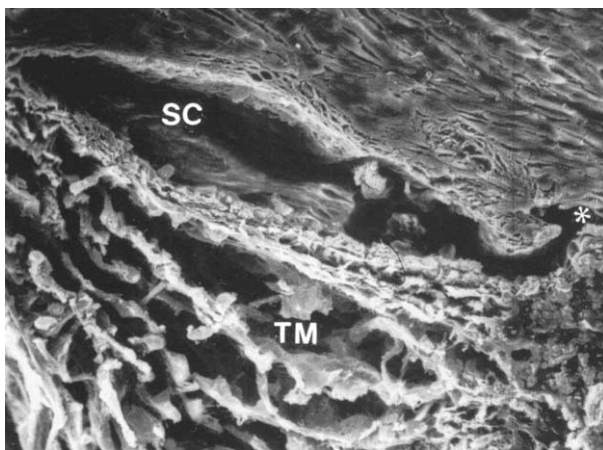


Fig. 1. Scanning electron micrograph of trabecular meshwork (TM) and Schlemm's canal (SC) from a human eye. Both regions are more expanded than they would be under physiological conditions. Asterisks shows a collecting channel (Freddo, 1993 (and revised 1999)). © 1993, Appleton and Lange.

glaucomatous condition worse, but it could not cause the glaucoma.

Upon leaving Schlemm's canal, the aqueous humour enter one of approximately 30 collecting channels that connect Schlemm's canal with the aqueous veins. The collector channels and aqueous veins have diameters that are tens of microns across. (Dvorak-Theobald, 1934; Batmanov, 1968; Rohen and Rentsch, 1968; Rosenquist et al., 1989) Use of Poiseuille's law leads to the conclusion that these vessels should have negligible flow resistance. (Rosenquist et al., 1989)

The experimental support for this conclusion is mixed. Mäpea and Bill (1989, 1992) measured pressures in Schlemm's canal of primate eyes and found the pressure there little different from episcleral venous pressure. This is in agreement with the theoretical calculations. However, a number of investigators (Grant, 1958, 1963; Ellingsen and Grant, 1972; Van Buskirk and Grant, 1973; Peterson and Jocson, 1974; Van Buskirk, 1977) have perfused enucleated primate and human eyes before and then after a 360° trabeculotomy, which would be expected to eliminate all flow resistance proximal to the collector channels and aqueous veins. All of these studies have shown that at least 25% of outflow resistance remains after this procedure, in contrast to what would have been predicted theoretically.

These disparate experimental results regarding the flow resistance of the collector channels and aqueous veins have not been reconciled, perhaps due to the fact that while a significant fraction of normal aqueous humour outflow resistance may be generated by the collector channels and/or aqueous veins, these vessels are not responsible for the elevated outflow resistance characteristic of the glaucomatous eye. Several observations lead to this conclusion. First, in a early study by Grant (1963), a trabeculotomy eliminated all of the elevated glaucomatous flow resistance in eight glaucomatous eyes. This result indicated that in primary open-angle glaucoma, the outflow obstruction is proximal to the collector channels and aqueous veins. Further support for this conclusion can be found in the success of laser trabeculoplasty (LTP) in reducing outflow resistance in glaucomatous eyes (Wise and Witter, 1979). While it is not known precisely what locus in the outflow pathway LTP acts upon, recent evidence suggest that the site of action is in the trabecular meshwork, (Van Buskirk et al., 1984; Bradley et al., 2000; Johnson and Erickson, 2000) and it seems very unlikely that LTP has an significant effect on the outflow resistance of the collector channels and/or aqueous veins.

The considerations detailed in this section indicate that little if any significant flow resistance in the normal eye is found in the uveal meshwork, corneoscleral meshwork, Schlemm's canal, or the collector channels and aqueous veins. While some increased resistance might be found in these structures in the glaucomatous eye, they are not responsible for the bulk of the elevated outflow resistance characteristic of the glaucomatous eye. The focus of this review now turns to the region immediately surrounding the inner wall of Schlemm's canal where all evidence indicates that normal aqueous humour outflow resistance resides, and where the elevated flow

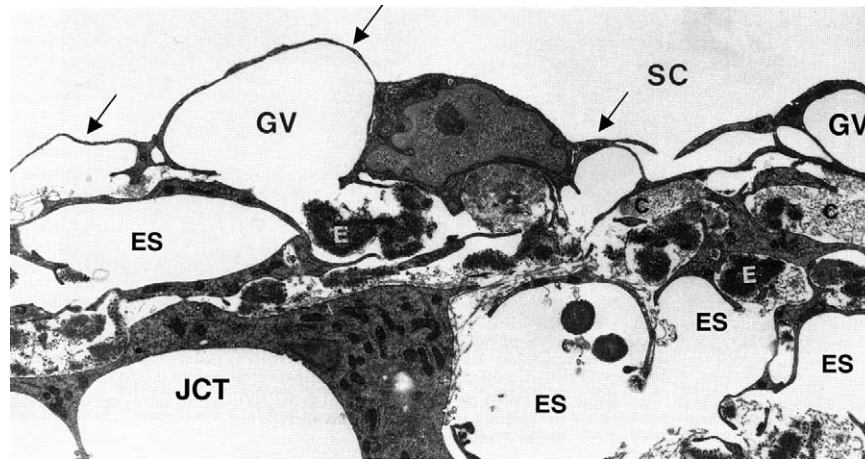


Fig. 2. Transmission electron micrograph of the inner wall of Schlemm's canal (SC) of a human eye, showing the endothelium (arrows) and giant vacuoles within this endothelial layer (GV). The region immediately below the inner wall and basement membrane is the juxtacanalicular connective tissue (JCT) and has many large, apparently empty spaces (ES). Collagen (C) and elastin (E) are apparent in the JCT along with fibroblastic-like cells. Magnification in source article  $\times 89,100$  (Gong et al., 1996). © 1996, Wiley-Liss, Inc.

resistance characteristic of primary open-angle glaucoma also likely arises.

## 2. The inner wall region of Schlemm's canal

Here, the term 'inner wall region' is used to refer to the inner wall endothelium of Schlemm's canal, its basement membrane and the adjacent juxtacanalicular connective tissue. Fig. 2 shows a transmission electron micrograph of the tissues that neighbours Schlemm's canal on its upstream side.

The endothelial lining of inner wall of Schlemm's canal is typical in some ways of other vascular linings. (Tripathi, 1974a, b) The cells are long, flattened cells that are spindle-shaped with a central nuclear bulge and tapering rounded edges. Their long axis is parallel to the canal (in the direction of flow through the canal) with a length of 40–100  $\mu\text{m}$  and a width of 5–15  $\mu\text{m}$ . They are flattened cells with a thickness of 1  $\mu\text{m}$  or less, except in their nuclear region. They are attached to one another with tight junctions (Raviola and Raviola, 1981; Bhatt et al., 1995).

This endothelium has several unique characteristics. First, structures known as 'giant vacuoles' are seen in this layer. (Fig. 3) While they appear to be intracellular structures, they are really outpouchings of the endothelium into Schlemm's canal, caused by the pressure drop across inner wall endothelial cells (Brilakis and Johnson, 2001). Epstein and Rohen (1991) described these structures as 'dilations of the paracellular spaces'. Grierson and Lee (1978) showed that these structures were invaginations into the canal with most having a large opening on the meshwork side of the vacuole. Twenty to thirty percent of these vacuoles also have a distal opening, a pore, and thus some of the vacuoles are transcellular channels.

It has not always been sufficiently appreciated that cell processes from the inner wall endothelium are frequently attached to a second layer of cells (Fig. 4). This layer was first

noted by Holmberg (1959, 1965) who considered the inner wall of Schlemm's canal 'to be formed by two endothelial layers separated by a narrow space'. Two distinct layers are only apparent in eyes fixed by immersion; this distinction is lost in eyes fixed by perfusion. Only the outer layer (the endothelial lining of the inner wall of Schlemm's canal) is continuous. Cell processes from the cells of this endothelium attach to the inner layer of cells that have been called subendothelial cells, (Johnstone, 1979) but whose cell type has not yet been determined. This latter layer is, in some cases, responsible for the impression that giant vacuoles appear to be intracellular structures since this layer can sometimes make up the basal aspect of some vacuoles (see (Epstein and Rohen, 1991)).

The distal openings, or pores, in these vacuoles are a second feature of the inner wall endothelium that is relatively unique (Fig. 3). The majority of these pores are transcellular, although a fraction of these pores are located at the border of two cells (border pores), and thus not transcellular (Ethier et al., 1998). The transcellular pores do not connect the extracellular fluid

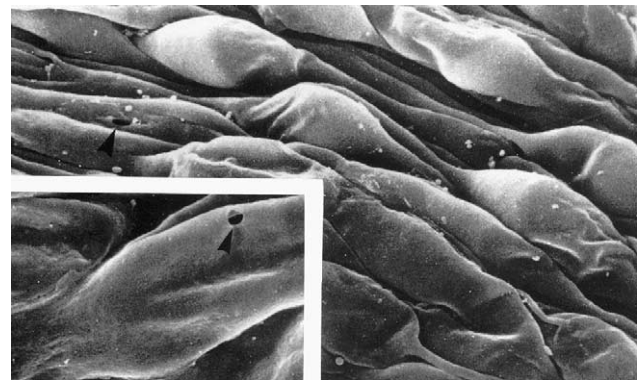


Fig. 3. Scanning electron micrograph of the inner wall of Schlemm's canal as viewed from within the canal. The bulging structures are giant vacuoles (and some nuclei). The insert shows an arrowhead pointing at a pore passing through one of the giant vacuoles (modified from (Allingham et al., 1992)). © 1992, Association for Research in Vision and Ophthalmology.



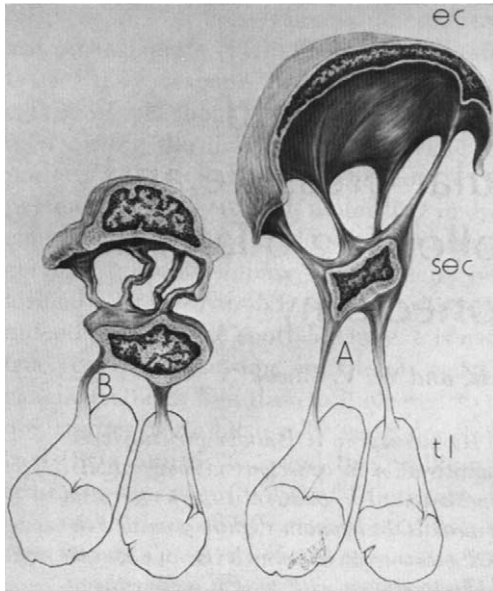


Fig. 4. Schematic diagram showing change in configuration of cell (EC) of endothelial lining of Schlemm's canal going from low IOP (B) to high IOP (A). These cells attach to a second layer of cells (SEC) that in turn attach to the trabecular lamella (tl). (Johnstone, 1979). © 1979, Association for Research in Vision and Ophthalmology.

with the cytoplasm of the cell. Instead, they pass from the basal side of the cell to the apical side at a location on the cell surface where the cell membranes from the inner and outer surfaces of the cell have come together and fused. The pore is thus membrane-lined on its surface. These pores usually form on giant vacuoles since it is in this region in which the cell is greatly attenuated and the cytoplasm becomes thin.

Fusion of the inner and outer cell membranes and the formation of transcellular pores are not entirely unique to these cells. Pores associated with giant vacuoles are also found on the arachnoid villi in the drainage pathway for the cerebrospinal fluid (Tripathi, 1974a,b, 1977; Angevine, 1994). When cell thickness is reduced below a critical thickness, vascular

endothelium can form transcellular pores involved in transport processes (Palade et al., 1979; Neal and Michel, 1995; Neal and Michel, 1996; Savla et al., 2002).

The inner wall endothelium of Schlemm's canal is supported by a discontinuous basement membrane. This makes Schlemm's canal a somewhat unique vessel having a continuous endothelium with tight junctions between neighbouring cell, supported by a discontinuous basement membrane. Blood vessel endothelia have a continuous endothelium with a continuous basement membrane, while lymphatics have a discontinuous endothelium with a discontinuous basement membrane (Gong et al., 1996).

The region immediately underlying the inner wall and basement membrane is the juxtacanalicular connective tissue (JCT) and has many large, apparently empty spaces. This region extends from the last trabecular beam until the basement membrane of the inner wall endothelium. It is typically 2–15  $\mu\text{m}$  thick. The JCT is more porous (30–40% open space when fixed under flow conditions) (Ten Hulzen and Johnson, 1996) than most other connective tissues.

The JCT has extracellular matrix components typical of connective tissues and fibroblastic-like cells that lack a basal lamina (Gong et al., 1996) but that are connected to the extracellular matrix with integrins (Tervo et al., 1995). The extracellular matrix components include collagen types I, III, IV, V and VI (but not type II), (Lütjen-Drecoll et al., 1989; Marshall et al., 1990; Marshall et al., 1991) elastin, (Gong et al., 1989) laminin, (Marshall et al., 1990) fibronectin, (Gong et al., 1996) and glycosaminoglycans, particularly dermatan sulfate, chondroitin sulfate and hyaluronic acid (Gong et al., 1996). With aging, this region shows an accumulation of structures called plaques (Lütjen-Drecoll et al., 1981; Alvarado et al., 1986). In glaucoma, there appears to be an increased age-related accumulation of plaque material, although this accumulation has little hydrodynamic consequence, as mentioned below.

### 3. The generation of flow resistance in the inner wall region of Schlemm's canal

While there is agreement among most investigators that the bulk of aqueous humour outflow resistance is generated in the immediate vicinity of the inner wall endothelium of Schlemm's canal, the precise location and the mechanism by which this dissipation occurs is still a topic of active debate and research.

#### 3.1. The juxtacanalicular connective tissue (JCT)

The JCT, with its tortuous submicron-sized flow pathways, is a natural location to investigate as to its role in generating outflow resistance. Surprisingly, morphometric analysis combined with theoretical calculations have indicated that, unless these apparently open spaces are actually filled with an extracellular matrix gel, they would generate an insignificant fraction of the total outflow resistance (Kamm et al., 1983; Seiler and Wollensak, 1985; Ethier et al., 1986).

Table 1  
Specific hydraulic conductivity ( $K$ ) of connective tissues

Tissue	$K \times 10^{14} (\text{cm}^2)$
Lens capsule <sup>a</sup>	0.1
Descemet's membrane <sup>b</sup>	0.1–0.2
Bruch's membrane <sup>c</sup>	0.5–1.5
Glomerulus basement membrane <sup>d</sup>	2
Aortic wall <sup>e</sup>	0.5–2.5
Corneal stroma <sup>c</sup>	0.5–2.5
Sclera <sup>c</sup>	1.4
Cartilage <sup>f</sup>	1–10
Synovium <sup>g</sup>	1.5–7
Vitreous humor <sup>h</sup>	1500–1800

<sup>a</sup> Fels (1970).

<sup>b</sup> Fatt (1969).

<sup>c</sup> Starita et al. (1997).

<sup>d</sup> Robertson and Walton (1989).

<sup>e</sup> Levick (1987).

<sup>f</sup> Mow et al. (1984).

<sup>g</sup> Levick et al. (1996)

<sup>h</sup> Fatt (1977).

This conclusion was reached using porous media theory to characterize the flow resistance of the JCT, an approach that has been used in other connective tissues (Levick, 1987). Several different parameters can be used to characterize the fluid transport capacity of a tissue. The flow resistance ( $R = \Delta P/Q$ ) of a tissue is the ratio between the pressure drop across that tissue ( $\Delta P$ ) and the flow rate generated by that pressure drop ( $Q$ ); the inverse of this quantity is known as the total hydraulic conductance of this tissue. The conductance per unit surface area is known as the hydraulic conductivity ( $L_p$ ), while the conductance of the tissue normalized for surface area, tissue length in the flow wise direction ( $L$ ) and fluid viscosity ( $\mu$ ) is known as the specific hydraulic conductivity ( $K$ ).

Darcy's law relates the flow resistance ( $R$ ) of a tissue to the specific hydraulic conductivity ( $K$ ) of that tissue,

$$R = \frac{\Delta P}{Q} = \frac{\mu L}{KA} \quad (1)$$

and the specific hydraulic conductivity is related to the hydraulic conductivity as:

$$K = L_p \mu L \quad (2)$$

Typical values of  $K$  and  $L_p$  for a variety of tissues are found in Tables 1 and 2.

The  $K$  value that characterizes the flow resistance of a tissue can be measured experimentally by determining the other parameters in Eq. (1), all of which are easy to determine or estimate for aqueous humour outflow with the exception of the length ( $L$ ) over which the pressure drop occurs. However, since the bulk of the pressure drop occurs somewhere in or near the inner wall of Schlemm's canal, it can be concluded that this length is less than roughly 10  $\mu\text{m}$ , or so, an estimate supported by experimental studies (Maepea and Bill, 1992). Using a flow rate through the aqueous outflow pathway of 2  $\mu\text{l}/\text{min}$  passing through a cross-sectional area of between 0.054 and 0.13  $\text{cm}^2$  (canal width of 150–350  $\mu\text{m}$ ; canal length

Table 2  
Hydraulic conductivity ( $L_p$ :  $\text{cm}^2 \text{ sec}^{-1} \text{ g}^{-1}$ ) for a variety of physiological membranes

Membrane	Type <sup>a</sup>	$L_p \times 10^{11}$
Kidney epithelial cells (MDCK cells) <sup>b</sup>	<b>a</b>	0.075
Xenopus oocytes <sup>c</sup>	<b>a</b>	0.2
Xenopus oocytes + CHIP28 <sup>c</sup>	<b>a</b>	1.6
Proximal tubule epithelial cells <sup>d</sup>	<b>a</b>	1.2
Red blood cells <sup>d,e</sup>	<b>a</b>	1–1.6
Gall bladder epithelial cells <sup>f</sup>	<b>a</b>	4–9
Corneal epithelium <sup>g,h</sup>	<b>b</b>	0.04–0.7
Gall bladder epithelium <sup>d,f</sup>	<b>b</b>	1.3–3.6
Proximal tubule epithelium <sup>b,d</sup>	<b>b</b>	7.5–55
Retinal pigment epithelium <sup>i</sup>	<b>b</b>	16
Brain capillary <sup>j</sup>	<b>c</b>	0.03
Corneal endothelium <sup>g,k</sup>	<b>c</b>	0.14–5
Lung capillary <sup>j</sup>	<b>c</b>	3.4
Skeletal muscle capillary <sup>j,l</sup>	<b>c</b>	2.5–7
Cardiac muscle capillary <sup>j,l</sup>	<b>c</b>	8.6
Aorta <sup>m</sup>	<b>c</b>	9
Mesentery, omentum <sup>l</sup>	<b>c</b>	50
Intestinal mucosa <sup>i,l</sup>	<b>d</b>	32–130
Synovium (knee) <sup>l</sup>	<b>d</b>	120
Renal peritubular capillaries <sup>l</sup>	<b>d</b>	225–700
Renal glomerulus <sup>i,l</sup>	<b>d</b>	400–3100
Descemet's membrane <sup>h</sup>	<b>e</b>	15–37
Lens capsule <sup>n</sup>	<b>e</b>	17–50
Bruch's membrane <sup>o</sup>	<b>e</b>	2000–12 500
Kidney tubule basement membrane <sup>p</sup>	<b>e</b>	6300–13 700

<sup>a</sup> **a**, cell membranes; **b**, unfenestrated epithelium; **c**, unfenestrated endothelium; **d**, fenestrated epithelia; and **e**, basement membranes.

<sup>b</sup> Timbs and Spring (1996).

<sup>c</sup> Preston et al. (1992).

<sup>d</sup> Gonzalez et al. (1982).

<sup>e</sup> Solomon et al. (1983).

<sup>f</sup> Persson and Spring (1982).

<sup>g</sup> Klyce and Russell (1979).

<sup>h</sup> Fatt (1969).

<sup>i</sup> Tsuboi (1987).

<sup>j</sup> Renkin (1977).

<sup>k</sup> Hedbys and Mishima (1962).

<sup>l</sup> Levick and Smaje (1987).

<sup>m</sup> Vargas et al. (1979).

<sup>n</sup> Fisher (1982).

<sup>o</sup> Starita et al. (1996) (eyes under 40) and Bentzel and Reczek (1978).

<sup>p</sup> Welling and Welling (1978).

around the eye of 3.6 cm (Ten Hulzen and Johnson, 1996)), and a pressure drop of 5 mmHg, it can then be determined that  $K$  for the resistance-causing region in the aqueous outflow pathway must be less than  $65 \times 10^{-14} \text{ cm}^2$ . Unless the length over which the pressure drop occurs ( $L$ ) is much smaller than  $10 \mu\text{m}$ , the specific hydraulic conductivity of the connective tissue elements in the outflow pathway is greater than that of any other connective tissue with the exception of the vitreous humour (Table 1).

$K$  can also be estimated from photomicrographs showing the ultrastructure of a tissue (Overby et al., 2001). This can potentially allow an evaluation of which structures in the aqueous outflow pathway are generating the measured outflow resistance. Carmen–Kozeny theory relates the structure of a porous medium to  $K$  as:

$$K = \frac{\varepsilon D_h^2}{80} \quad (3)$$

where  $D_h$  is the hydraulic diameter of the open-spaces available for flow and  $\varepsilon$  is the porosity, or fraction of open space of the medium (note that at porosities higher than roughly 0.8, this equation becomes inaccurate). Using Carmen–Kozeny theory combined with conventional transmission electron microscopy, it was found (in immersion-fixed eyes) that the porosity of the JCT was approximately 0.15–0.25,  $D_h$  was approximately 1–1.5  $\mu\text{m}$ , and most importantly,  $K$  of the JCT was calculated to be approximately  $2000\text{--}10\,000 \times 10^{-14} \text{ cm}^2$  based on the photomicrographs (Ethier et al., 1986; Murphy

et al., 1992). This is, at least, thirty times greater than the measured  $K$  of the outflow system.

Based on this, Ethier et al. (1986) concluded that the JCT, as visualized using conventional transmission electron microscopy, could not generate a significant fraction of outflow resistance. Other investigators have confirmed this conclusion including studies in which the eyes were fixed by perfusion (Seiler and Wollensak, 1985; Murphy et al., 1992; Ten Hulzen and Johnson, 1996). It thus followed that either this region was filled with an extracellular matrix gel that was poorly visualized using conventional TEM techniques, or, that this region was not the primary site of outflow resistance. The age-related accumulation of ‘plaque-like material’ in this region that is enhanced in glaucomatous would have no influence on this conclusion (Alvarado et al., 1986; Murphy et al., 1992).

More recently, Gong et al. (2002) used the quick-freeze/deep-etch methodology to examine the apparent open spaces seen in the JCT region in greater detail. QFDE is a morphological technique that preserves the cellular and extracellular ultrastructure in exquisite detail and allows visualization of structures poorly preserved or not seen at all using conventional TEM tissue preparation techniques (Mecham and Heuser, 1990; Kubosawa and Kondo, 1994). A more elaborate and extensive extracellular matrix was seen in the JCT using QFDE as compared to conventional methods of preparation for TEM (Fig. 5); however, micron-sized open spaces were still seen in this region, casting doubt on whether a significant fraction of outflow resistance could be generated in

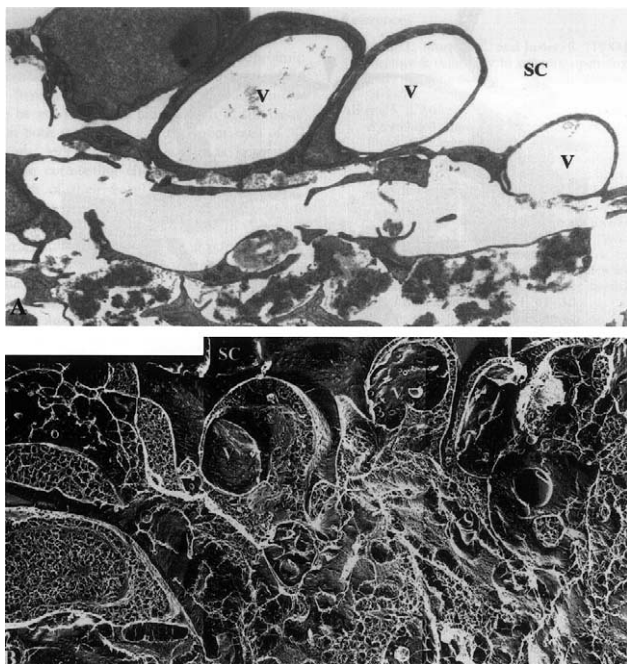


Fig. 5. Enucleated human eye fixed by perfusion at 15 mmHg: (A) vacuoles (V) in the inner wall of Schlemm's canal (SC) in tissue prepared for TEM using conventional methods; notice the large open space in the region of the JCT immediately under these vacuoles; (B) the same region as seen in tissue prepared using QFDE; notice that while open spaces still exist under the vacuoles, a more complex and extensive extracellular matrix is seen ( $\times 4860$ ) (Gong et al., 2002). © 2002, Elsevier.

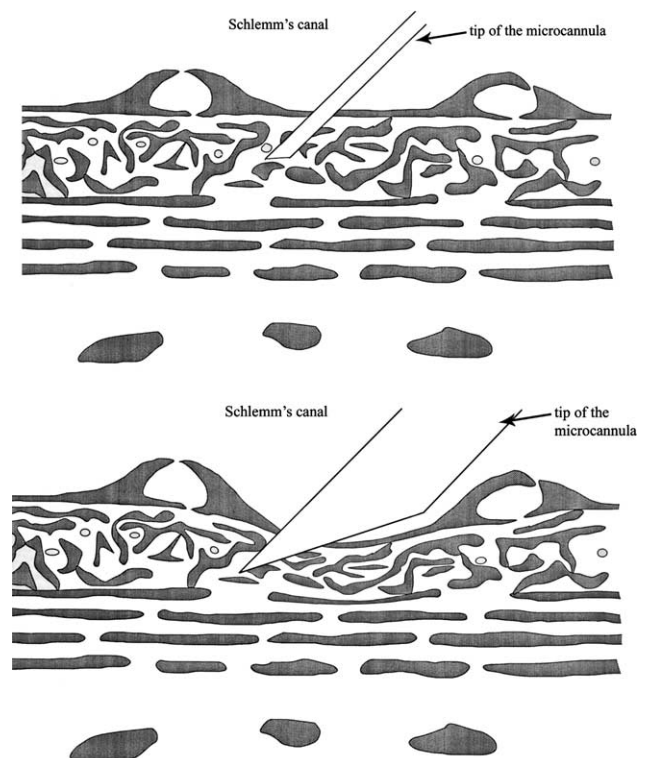


Fig. 6. (A) Schematic of use of micropipette to measure pressure in JCT as described by Maepea and Bill; (B) corrected schematic showing realistic size of micropipette in the JCT. Revised from (Maepea and Bill, 1992). © 1992, Elsevier.



this region. An important caveat pointed out by Gong et al. regarding their studies was that it was not clear whether or not QFDE can visualize the glycosaminoglycans in their uncollapsed state, and this uncertainty leaves the question of generation of appreciable flow resistance in the JCT region in doubt.

The role that glycosaminoglycans and other extracellular matrix elements found in the JCT might play in generating outflow resistance is unclear. While it has been shown that enzymes that degrade glycosaminoglycans (GAGases) increase outflow facility in a number of species (cow, guinea pig, dog, rabbit), the evidence regarding primates is conflicting, and there has been no confirmed data yet showing that GAGases decrease outflow resistance in human eyes (Johnson and Erickson, 2000). Matrix metalloproteinases (MMPs) have been shown to reversibly increase outflow facility in perfused human anterior segment organ culture, and this is a strong indicator that the extracellular matrix may generate significant aqueous outflow resistance (Bradley et al., 1998).

Perhaps the strongest experimental evidence implicating the JCT as a major site of outflow resistance is the study of Maepea and Bill, (1992) in which micropipettes were used to localize the pressure drop to occurring between 7 and 14  $\mu\text{m}$  from the inner wall of Schlemm's canal. While this result is frequently cited in the literature, it is not widely appreciated that this measurement was made with a device whose tip size was as large as the measurement zone. Fig. 6A shows the schematic of the measurement device in situ as given in the Maepea and Bill paper, while Fig. 6B, shows a corrected schematic with the measurement device drawn roughly to scale. When this reservation is combined with the fact that the inner wall of Schlemm's canal distends several to many micrometers during the process of penetration by the micropressure probe (unpublished work by Dr Milko Iliev in collaboration with our laboratory), it leads to the conclusion that the bulk of the aqueous humour pressure drop occurs near the inner wall of Schlemm's canal (within 5–10  $\mu\text{m}$ ), but that no further quantitative conclusions are possible.

### 3.2. The basement membrane

The other possible loci for generation of outflow resistance are the basement membrane of the inner wall of Schlemm's canal, and the inner wall endothelium itself. The basal lamina or 'basement membrane' has the potential to generate a significant flow resistance. Table 1 shows that the specific hydraulic conductivities of basement membranes (top four tissues in table) are among the lowest of connective tissues.

However, basal lamina tend to be quite thin and this limits the flow resistance they can generate (see Eq. (1)). Table 2 shows the hydraulic conductivity of a variety of physiological membranes, including cell membranes, epithelia and basement membranes. The large variation in  $L_p$  of basement membranes is due not only to variation in the specific hydraulic conductivity of these tissues, but also to significant differences in their thicknesses (ranging from 0.15  $\mu\text{m}$  for Bruch's

membrane (Marshall et al., 1998) to 7  $\mu\text{m}$  for Descemet's membrane (Fatt, 1969)).

It is interesting to compare the values seen in this table with the estimated value of the hydraulic conductivity of the outflow pathway. From the definition of hydraulic conductivity (or by combining Eqs. (1) and (2)),  $L_p = Q/A/\Delta P$ . Using the values characterizing the aqueous outflow pathway presented above, we can estimate that  $L_p$  for the aqueous humour outflow pathway is between  $4000 \times 10^{-11}$  and  $9000 \times 10^{-11}$   $\text{cm}^2 \text{ sec/g}$ . Note that this is not a theoretical calculation but an estimate based on measured quantities.

In Table 2, we see that several basement membranes, in particular those of the renal system, have hydraulic conductivities similar to that of the aqueous outflow pathway. This suggests that the basement membrane of the inner wall endothelium of Schlemm's canal might be an important contributor to aqueous humour outflow resistance.

However, as noted above, this basement membrane is unique (as compared with vascular basement membranes) in that it is discontinuous. The recent study by Gong et al. (2002) examining the inner wall region using quick-freeze/deep-etch appeared to confirm this conclusion. If there are breaks in the basement membrane, it is difficult to see how a significant flow resistance could be generated by this tissue.

### 3.3. The inner wall endothelium of Schlemm's canal

Since the time that light microscopes and later electron microscopes have been focused on the inner wall endothelium, this tissue has been an attractive candidate for the generation of aqueous humour outflow resistance. However, to appreciate the role of this tissue in generating outflow resistance, it must be recognized that, as best as is currently understood, all conventional aqueous humour outflow must pass through this cellular lining. As such, comparison of the hydraulic conductivity of this tissue ( $4000\text{--}9000 \times 10^{-11}$   $\text{cm}^2 \text{ sec/g}$ ) with that of other endothelia and epithelia as seen in Table 2, leads one to conclude that this vessel lining must have one of the highest hydraulic conductivities in the body. Compared to other tissues in Table 2, it is clear that only fenestrated endothelia (and some basement membranes) have such high hydraulic conductivities.

While the inner wall endothelium is not fenestrated, this endothelium is unique in that it contains micron-sized pores. It is interesting that even early investigators had concluded the such pores existed (Seidel, 1921), long before they were first seen by electron microscopy (Garron et al., 1958; Holmberg, 1959; Speakman, 1959). This conclusion was based on early filtration studies that examined the sizes of microparticulates that would pass through the outflow pathway. It was found in these studies that a filtration barrier existed for particles larger than roughly one half micrometer or so, and thus it was concluded that pores nearly one micrometer in size must exist. More recent studies have confirmed this conclusion using microparticles and latex microspheres (Huggert, 1955; Huggert et al., 1955; Karg et al., 1959; Johnson et al., 1990).

While there is some debate concerning the existence of these pores (which is discussed below), no group has offered an alternate explanation for the extraordinarily high hydraulic conductivity of the aqueous outflow pathway. Nor has any alternate explanation been offered for the relatively easy passage of microparticles 200–500 nm in diameter through the outflow pathway (Johnson et al., 1990), except through these large pores. Since there are intact tight junctions between the inner wall cells (presumably to prevent blood reflux into the eye that can occur during periods of transient increases in ocular venous pressure), there are no other structures apparent in this endothelium that could explain the high hydraulic conductivity of this tissue or its filtration characteristics.

The flow resistance generated by these pores was first considered by Bill and Svedbergh (1972). In an exhaustive study using scanning electron microscopy, they characterized the size distribution of these pores, and then used hydrodynamic theory to calculate for hydraulic conductivity of these pores. Using Sampson's law, that gives the hydraulic conductivity for a single pore of diameter  $d$ ,

$$L_p = \frac{d}{6\pi\mu} \quad (4)$$

They found that the inner wall endothelium could present, at most, 10% of the outflow resistance. That is, the hydraulic conductivity of the pores in the inner wall endothelium is, at least, 10-fold higher than the measured hydraulic conductivity of the outflow pathway. This conclusion has been confirmed in a number of studies (Grierson et al., 1979; Eriksson and Svedbergh, 1980).

These results would appear to rule out the inner wall endothelium as a major site of outflow resistance. However, a number of experimental findings are at variance with this conclusion. In particular, when chelating agents (EDTA, EGTA: (Bill et al., 1980; Hamanaka and Bill, 1987)) or a proteolytic enzyme ( $\alpha$ -chymotrypsin: (Hamanaka and Bill, 1987)) were perfused through the outflow pathway of live primates, it was found that ruptures of the inner wall endothelium were produced by these agents that decreased outflow resistance more that could be explained by the calculated flow resistance of the inner wall pores.

It has been pointed out (Johnson et al., 1992) that a hydrodynamic interaction ('the funnelling effect') between the inner wall pores and the JCT, that lies immediately below these

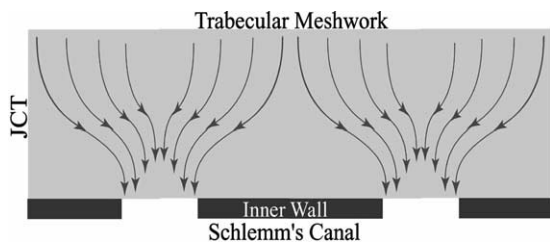


Fig. 7. Schematic of the 'funnelling' of aqueous humour through the JCT, toward a vacuole and pore that allows this fluid to pass through the inner wall endothelium (Overby et al., 2002). © 2002, Association for Research in Vision and Ophthalmology.

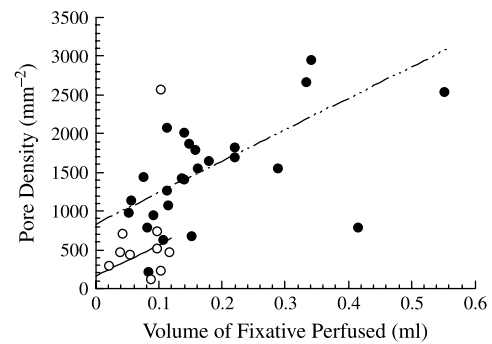


Fig. 8. Pore density as a function of volume of fixative perfused through the outflow pathway of normal eyes (filled symbols) and eyes with POAG (open). Lines are best fit with outliers excluded. Details in Johnson et al. (2002). © 2002, Association for Research in Vision and Ophthalmology.

pores, might explain the findings of Hamanaka and Bill (see Fig. 7). In this scenario, the pores and vacuoles themselves contribute negligible flow resistance, but since they force the fluid to 'funnel' through those regions of the JCT nearest the pores and vacuoles, the vacuole size and pore density can have a significant effect on the effective hydraulic conductivity ( $L_p$ ) of the JCT:

$$L_p = \frac{2KnD}{\mu} \quad (5)$$

here,  $K$  is the specific hydraulic conductivity of the JCT region,  $n$  is the number of pores per unit area in the inner wall,  $D$  is the diameter of the vacuoles in the inner wall and  $\mu$  is the viscosity of the aqueous humour.

The funnelling model suggests that while the bulk of outflow resistance is actually generated in the JCT, its magnitude is modulated by the pores and vacuoles of the inner wall endothelium of Schlemm's canal. This model explains many of the characteristics of the outflow pathways discussed above. However, two recent studies (Sit et al., 1997; Ethier et al., 1998) failed to find a correlation between outflow facility and inner wall pore density as would be expected if Eq. (5) describes the hydraulic conductivity of the outflow pathway. Furthermore, these studies found that at least some inner wall pores may be artifacts of the fixation process.

### 3.4. Pores as possible fixation artifacts and the possible importance of flow through inner wall cell junctions or through water channels

The micron-sized pores that pass through the endothelial cells of the inner wall endothelium of Schlemm's canal are relatively unique to these cells and to the cells of the arachnoid villi, a tissue of the cerebrospinal fluid pathway. This unique character has led some investigators to doubt that these are physiologic structures, but instead consider them to be artifacts of the tissue preparation process. The possibility that pores form during tissue preparation for electron microscopy was supported in recent studies that showed that during tissue fixation under flow conditions, the pore density of the inner wall endothelium increased as a function of the volume of



fixative perfused through the outflow pathway (see Fig. 8) (Sit et al., 1997; Ethier et al., 1998).

It has been postulated by several investigators (Epstein and Rohen, 1991; Alvarado et al., 1998; Brandt and O'Donnell, 1999; Underwood et al., 1999; Rao et al., 2001; Heimark et al., 2002) that instead of passing through the pores in the inner wall endothelium, a significant fraction of the aqueous humour passes through gaps between the tight junction strands of these cells. Ethier and Chan (Ethier and Chan, 2001) found that cationized ferritin perfused into enucleated human eyes acted to decreased outflow facility and was seen accumulating near junctions between inner wall endothelial cells. While Ethier and Chan argue that the decreased outflow facility caused by cationized ferritin was due to pore blocking that was also seen to occur in this study, others (Burke et al., 2004) have interpreted their results as consistent with a significant flow through the junctional complexes.

There are a variety of reasons why this hypothesis is untenable. Two strong argument against this possibility were already given above, namely that the uniquely high hydraulic conductivity of the aqueous outflow pathway is inconsistent with flow through intact tight junctions, and that the relatively free passage of microspheres 200–500 nm in diameter through the outflow pathway would be precluded if transport was primarily through such cell junctions. It is well known in the vascular system that macromolecules larger than roughly 10–20 nm are largely excluded from passing through intact tight junctions, for either fenestrated or non-fenestrated vessels (Pappenheimer et al., 1951; Simionescu et al., 1978; Curry, 1980; Bundgaard, 1984; Curry, 1984; Fu, 2001).

Raviola and Raviola (1981) examined the tight junctions of the inner wall endothelium and calculated the flow that would be expected through these junctions. The gaps they found available for transport around the tight junctional strands were nanometers in size, and they concluded that any flow that might occur through these spaces would be negligible. Ye et al. (1997) used freeze-fracture techniques to examine these junctions in eyes fixed under flow conditions and did not report significant differences from the dimensions reported by Raviola and Raviola. The notion that microparticles that are roughly one half micron in size could relatively easily pass through such openings seems improbable, at best.

The study of Ye et al. (1997) did find that the tight junctions of the inner wall cells simplified with increasing intraocular pressure. They speculated that the junctional simplification that occurred with increasing perfusion pressure might lead to border pore formation at locations of focal separation in the tight junctions. While they did not find a statistically significant relationship between junctional complexity and outflow facility in this small series of eyes, they did find a trend in that direction, consistent with their hypothesis.

Thus, while there are a number of strong arguments against the possibility of transport of a significant quantity of aqueous humour across the inner wall of Schlemm's canal passing directly through intact cell junctions, simplification of these junctions might be involved in the process of border pores

formation. Paracellular flow through border pores could be consistent with the findings of Epstein and Rohen (1991).

It has also been suggested that a fraction of aqueous humour outflow might pass through water channels (aquaporins) in the cell membrane of the inner wall cells (Stamer et al., 1995). Red blood cells and renal proximal tubules are cell types expressing high levels of aquaporin 1 (Preston et al., 1992). The hydraulic conductivities of the water channels in these cell membranes have been measured, as have those of cells in which aquaporins are overexpressed (see Table 2). All of these values are more than 1000 times smaller than the hydraulic conductivity of aqueous outflow pathway. It goes without saying that water channels also cannot explain the relatively free passage of half micron-sized particles through the outflow pathway.

The only pathway that appears consistent with the available physiologic evidence is through the inner wall pores whose existence was postulated already some 80 years ago (Seidel, 1921), and that now are easily seen using scanning electron microscopy of this tissue. Importantly, the size of these pores is consistent with the predictions of Seidel (1921). Whether this transport is primarily through border pores or is also through the transcellular pores remains to be determined.

The question remains as to why the number of these pores increases during the fixation process, as shown in Fig. 8. A further finding of the studies of Sit et al. and Ethier et al. was that the number density of pores in the inner wall endothelium decreases as a function of post-mortem time, something not expected of an artifact. Instead, it may be that that fixation under flow conditions generates stresses in the inner wall due both to pressure-induced stretching of the inner wall of Schlemm's canal and also to shrinkage of the tissue following fixation (Johnson et al., 2002). Pressure-induced stress is likely what causes the formation of these pores under physiologic conditions. Then, fixative-induced pore formation might be an artifact associated with a physiological process, namely stress on the inner wall endothelium. In this scenario, the y-intercepts of the lines seen on Fig. 8 would then represent the true physiological pore density of normal and glaucomatous eyes, respectively. Importantly, Fig. 8 shows this density to be greatly reduced in glaucomatous eyes.

#### 4. Future work

While the evidence supporting the existence and importance of inner wall pores to aqueous humour outflow is strong, there have been no studies investigating the cellular processes by which such structures might originate, form, remain stable, and finally close. This is true for both transcellular pores and for border pores. For transcellular pores to allow flow without compromising the barrier between intracellular and extracellular fluids, there must be a fusion of the basal and apical surface of the cell. Neal and Michel have suggested that transcellular openings occur when cell thickness is reduced to a critical value (Neal and Michel, 1995; Neal and Michel, 1996; Savla et al., 2002).

Proteins from the cortex of the cytoskeleton likely are involved in stabilizing the pores that form at this fusion site,

and some cellular mechanism must exist for modulating the pore number density such that intraocular pressure is maintained. The biophysics of the pore formation process should be evaluated, and the cytoskeletal mechanics underlying the process of pore formation needs to be elucidated. Studies of experimental pore formation in vascular endothelium might provide useful information (Neal and Michel, 1995; Neal and Michel, 1996; Savla et al., 2002).

Giant vacuoles likely have an important role in this process. The cells of the inner wall endothelium are under large stresses due to the pressure gradient across them that acts to separate them from their underlying basement membrane and/or underlying cells. This is very different than in vascular endothelium where the pressure is always greater within the vessel than in the tissue surrounding it, and thus vascular cells are being pressed against their supporting basement membrane rather than being pulled away from it.

Schlemm's canal cells undergo tremendous deformations due to this stress, with the surface area of the cells increasing by as much as 50% as the vacuoles expand with increasing intraocular pressure (Ethier, 2002). These strains cause the cell to thin, pulling together the apical and basal surface of the cell, thus facilitating the fusion necessary to form a transcellular pore, and perhaps also initiating cellular process associated with this pore formation. These strains also lead to junctional simplification, and this likely facilitates formation of border pores. The magnitude of the pressure drop across these cells is not known. If the entire aqueous outflow pressure drop (IOP—episcleral venous pressure) acts across these cells, it is hard to see how these cells could withstand such a tremendous load. More likely, as suggested by the funnelling model, most of the pressure drop occurs upstream either in the JCT region or in the basal lamina, and a much smaller pressure drop (perhaps a fraction of a mmHg) occurs over these thin cells (Bill and Svedbergh, 1972). This would still be expected to produce large deformations. Biomechanical studies are needed to determine the ability of inner wall cells to maintain the stresses caused by the pressure drop across these cells, and how pore formation acts to redistribute these stresses.

Detailed studies of the cell biology of these processes require a model system that allows access to the surface of these cells and facilitates controlled perturbations. Such a model is likely best accomplished by cell culture studies in which Schlemm's canal cells are perfused from basal to apical side as they are physiologically. This is a difficult experimental condition to replicate due to the significant stresses that these cells must sustain without detachment. The first attempt at such a model was by Alvarado's group (Perkins et al., 1988), but they found that they needed to perfuse from in the opposite direction (apical to basal) to avoid separating their cells from their substratum. This was likely due to the relatively high pressure drop they used in their system (5 mmHg), which matches the pressure drop of the aqueous outflow pathway, but, as mentioned above, is likely significantly larger than the physiological pressure drop across the inner wall endothelium. Whereas live and enucleated eyes can be perfused with pressure drops as high

as 30 mmHg with relatively normal appearance of the inner wall endothelium (Johnstone and Grant, 1973; Lee and Grierson, 1975), this does not appear to be possible in Schlemm's canal cell cultures perfused in the basal to apical direction (Alvarado et al., 2004).

A second potential experimental concern with such studies has to do with the maturity of the junctions between the cells when the study is begun. Junctions between cells continue to mature long after the cells have become confluent (Albelda et al., 1988; Sill et al., 1992; Yaccino et al., 1997; Underwood et al., 1999; Kaida et al., 2000; Penfold et al., 2000). These studies have shown that the permeability to solutes, electrical resistance, and hydraulic conductivity can continue to change one to 2 weeks post confluence in endothelial monolayers. Measurements of hydraulic conductivity should only be made after the junctions become stable (Burke et al., 2004). This is especially a concern for studies using steroids or other agents that directly affect these junctions and thus can influence how long they take to become stable (Underwood et al., 1999). Maturity of the junctions should be confirmed by ascertaining that the hydraulic conductivity of such systems is indeed stable over an extended period of hours. It is likely that this will only be possible at very low pressure drops making these experiments technically challenging.

Recent results using these models have providing interesting findings, demonstrating that the hydraulic conductivity of these cells can change depending on whether the cells are perfused from the apical or basal side (Alvarado et al., 2004). Distinct differences in cell morphology are also seen depending on the perfusion direction (Alvarado et al., 2004). However, the cellular morphology of these systems do not yet match what is found physiologically. These *in vitro* cell layers show large (micro-sized) intercellular gaps (Underwood et al., 1999; Alvarado et al., 2004) that are not seen physiologically. The permeability of vascular monolayers are reported to be 10–100 times greater than for intact endothelia, presumably due to such defects (Albelda et al., 1988; Sill et al., 1992). Formation of large blebbing structures in the cells have also been seen when these cellular layers are perfused from the basal to apical direction (Alvarado et al., 2004), but these structures are different in size and morphological characteristics from giant vacuoles that are seen in Schlemm's canal cells from intact tissues (Bill, 1970; Johnstone and Grant, 1973; Ethier, 2002). Nonetheless, these studies provide the first glimpses at how these cells deal with a unique physiological stress environment. Dramatic insights into aqueous humour outflow dynamics are likely to come from such studies.

## Acknowledgements

Support was provided by NIH R01-EY09699. Permission to use Figure 1 was granted by Dr. Murray Fingeret. Figure 2 was reprinted with permission of Wiley-Liss, Inc. a subsidiary of John Wiley & Son, Inc. Figure 3, 4, 7 and 8 were reprinted with permission of the Association for Research in Vision and Ophthalmology. Figure 5 was reprinted with permission from

Elsevier. Figure 6 was modified and reprinted with permission from Elsevier.

## References

- Albelda, S.M., Sampson, P.M., et al., 1988. Permeability characteristics of cultured endothelial cell monolayers. *J. Appl. Physiol.* 64, 308–322.
- Allingham, R.R., de Kater, A.W., et al., 1992. The relationship between pore density and outflow facility in human eyes. *Invest. Ophthalmol. Vis. Sci.* 33 (5), 1661–1669.
- Alvarado, J.A., Yun, A.J., et al., 1986. Juxtacanalicular tissue in primary open angle glaucoma and in nonglaucomatous normals. *Arch. Ophthalmol.* 104, 1517–1528.
- Alvarado, J.A., Murphy, C.G., et al., 1998. Effect of beta-adrenergic agonists on paracellular width and fluid flow across outflow pathway cells. *Invest. Ophthalmol. Vis. Sci.* 39, 1813–1822.
- Alvarado, J.A., Betanzos, A., et al., 2004. Endothelia of Schlemm's canal and trabecular meshwork: distinct molecular, functional, and anatomic features. *Am. J. Physiol. Cell Physiol.* 286, C621–C634.
- Angevine, J., 1994. The nervous tissue. In: Bloom, W., Fawcett, D. (Eds.), *A Textbook of Histology*. Chapman & Hall, New York, pp. 363–364.
- Batmanov, Y.E., 1968. Structure of the eye drainage system in man. *Vestn. Oftalmol.* 4, 27–31.
- Bentzel, C., Reczek, P., 1978. Permeability changes in *Necturus* proximal tubule during volume expansion. *Am. J. Physiol.* 234, F225–F234.
- Bhatt, K., Gong, H., et al., 1995. Freeze-fracture studies of interendothelial junctions in the angle of the human eye. *Invest. Ophthalmol. Vis. Sci.* 36, 1379–1389.
- Bill, A., 1964a. The albumin exchange in the rabbit. *Acta Physiol. Scand.* 60, 18.
- Bill, A., 1964b. The drainage of albumin from the uvea. *Exp. Eye Res.* 3, 179.
- Bill, A., 1965. The aqueous humor drainage mechanism in the cynomolgus monkey (*Macaca irus*) with evidence for unconventional routes. *Invest. Ophthalmol.* 4, 911.
- Bill, A., 1970. Scanning electron microscopic studies of the canal of Schlemm. *Exp. Eye Res.* 10, 214.
- Bill, A., 1975. Blood circulation and fluid dynamics in the eye. *Physiol. Rev.* 55, 383–416.
- Bill, A., Hellsing, K., 1965. Production and drainage of aqueous humor in the cynomolgus monkey (*Macaca irus*). *Invest. Ophthalmol.* 4, 920.
- Bill, A., Mäepea, O., 1994. Mechanisms and routes of aqueous humor drainage. In: Albert, D.M., Jakobiac, F.A. (Eds.), *Principles and Practice of Ophthalmology Basic Sciences*, vol. I. Saunders, Philadelphia, PA (Chapter 12).
- Bill, A., Phillips, C.I., 1971. Uveoscleral drainage of aqueous humor in human eyes. *Exp. Eye Res.* 12, 275–281.
- Bill, A., Svedbergh, B., 1972. Scanning electron microscopic studies of the trabecular meshwork and the canal of Schlemm—an attempt to localize the main resistance to outflow of aqueous humor in man. *Acta Ophthalmol.* 50, 295–320.
- Bill, A., Lütjen-Drecoll, E., et al., 1980. Effects of intracameral Na<sub>2</sub>EDTA and EGTA on aqueous outflow routes in the monkey eye. *Invest. Ophthalmol. Vis. Sci.* 19, 492–504.
- Bradley, J.M.B., Vranka, J., et al., 1998. Effect of matrix metalloproteinases activity on outflow in perfused human organ culture. *Invest. Ophthalmol. Vis. Sci.* 39, 2649–2658.
- Bradley, J.M., Anderssohn, A.M., et al., 2000. Mediation of laser trabeculoplasty-induced matrix metalloproteinase expression by IL-1beta and TNFalpha. *Invest. Ophthalmol. Vis. Sci.* 41, 422–430.
- Brandt, J.D., O'Donnell, M.E., 1999. How does the trabecular meshwork regulate outflow? Clues from the vascular endothelium. *J. Glaucoma* 8, 328–339.
- Brilakis, H.S., Johnson, D.H., 2001. Giant vacuole survival time and implications for aqueous humor outflow. *J. Glaucoma* 10, 277–283.
- Brubaker, R.F., 1975. The effect of intraocular pressure on conventional outflow resistance in the enucleated human eye. *Invest. Ophthalmol. Vis. Sci.* 14, 286–292.
- Bundgaard, M., 1984. The three-dimensional organization of tight junctions in a capillary endothelium revealed by serial-section electron microscopy. *J. Ultrastruct. Res.* 88, 1–17.
- Burke, A.G., Zhou, W., et al., 2004. Effect of hydrostatic pressure gradients and Na<sub>2</sub>EDTA on permeability of human Schlemm's canal cell monolayers. *Curr. Eye Res.* 28, 391–398.
- Curry, F.E., 1980. Is the transport of hydrophilic substances across the capillary wall determined by a network of fibrous molecules? *Physiologist* 23, 90–93.
- Curry, F.E., 1984. Mechanics and thermodynamics of transcapillary exchange. In: Renkin, E.M., Michel, C.C. (Eds.), *Section 2: The Cardiovascular System*. American Physiology Society, Bethesda, MD (Chapter 8, IV: Microcirculation, Part 1).
- Dvorak-Theobald, G., 1934. Schlemm's canal: its anastomoses and anatomic relations. *Trans. Am. Ophthalm. Soc.* 32, 574–585.
- Ellingsen, B.A., Grant, W.M., 1972. Trabeculotomy and sinusotomy in enucleated human eyes. *Invest. Ophthalmol.* 11, 21–28.
- Epstein, D.L., Rohen, J.W., 1991. Morphology of the trabecular meshwork and inner-wall endothelium after cationized ferritin perfusion in the monkey eye. *Invest. Ophthalmol. Vis. Sci.* 32, 160–171.
- Eriksson, A., Svedbergh, B., 1980. Transcellular aqueous humor outflow: a theoretical and experimental study. *Graefes Arch. Clin. Exp. Ophthalmol.* 212, 187–197.
- Ethier, C.R., 2002. The inner wall of Schlemm's canal (REVIEW). *Exp. Eye Res.* 74, 161–172.
- Ethier, C.R., Chan, D.W., 2001. Cationic ferritin changes outflow facility in human eyes whereas anionic ferritin does not. *Invest. Ophthalmol. Vis. Sci.* 42, 1795–1802.
- Ethier, C.R., Kamm, R.D., et al., 1986. Calculations of flow resistance in the juxtacanalicular meshwork. *Invest. Ophthalmol. Vis. Sci.* 27, 1741–1750.
- Ethier, C.R., Coloma, F.M., et al., 1998. Two pore types in the inner wall endothelium of Schlemm's canal. *Invest. Ophthalmol. Vis. Sci.* 39, 2041–2048.
- Fatt, I., 1969. Permeability of Descemet's membrane to water. *Exp. Eye Res.* 8, 34–354.
- Fatt, I., 1977. Hydraulic flow conductivity of the vitreous gel. *Invest. Ophthalmol. Vis. Sci.* 16, 565–568.
- Fels, I.G., 1970. Permeability of the anterior bovine lens capsule. *Exp. Eye Res.* 10, 8–14.
- Fisher, R.F., 1982. The water permeability of basement membrane under increasing pressure: evidence for a new theory of permeability. *Proc. R. Soc. Lond. Ser. B* 216, 475–496.
- Freddo, T.F., 1993. Anatomy and physiology related to aqueous humor production and outflow. In: Fingeret, M., Lewis, T., Appleton, Lange (Eds.), *Primary Care of the Glaucomas*. Appleton and Lang, New York (Chapter 3).
- Fu, B.M., 2001. Microvessel Permeability and Its Regulation. *Recent Advances in Biomechanics*. Springer, Berlin, pp. 231–247.
- Garron, L.K., Fenney, M.L., et al., 1958. Electron microscopic studies of the human eye. *Am. J. Ophthalmol.* 46, 27–35.
- Gong, H.Y., Trinkaus-Randall, V., et al., 1989. Ultrastructural immunocytochemical localization of elastin in normal human trabecular meshwork. *Curr. Eye Res.* 8, 1071–1082.
- Gong, H., Tripathi, R.C., et al., 1996. Morphology of the aqueous outflow pathway. *Microsc. Res. Tech.* 33, 336–367.
- Gong, H., Ruberti, J., et al., 2002. A new view of the human trabecular meshwork using quick-freeze, deep-etch electron microscopy. *Exp. Eye Res.* 75, 347–358.
- Gonzalez, E., Carpi-Medina, P., et al., 1982. Cell osmotic water permeability of isolated rabbit proximal straight tubules. *Am. J. Ophthalmol.* 242, F321–F330.
- Grant, W.M., 1958. Further studies on facility of flow through the trabecular meshwork. *Arch. Ophthalmol.* 60, 523.
- Grant, W.M., 1963. Experimental aqueous perfusion in enucleated human eyes. *Arch. Ophthalmol.* 69, 783–801.
- Grierson, I., Lee, W.R., 1978. Pressure effects on flow channels in the lining endothelium of Schlemm's canal. *Acta Ophthalmol.* 56, 935–952.



- Grierson, I., Lee, W.R., et al., 1979. The trabecular wall of Schlemm's canal: a study of the effects of pilocarpine by scanning electron microscopy. *Br. J. Ophthalmol.* 63, 9–16.
- Hamanaka, T., Bill, A., 1987. Morphological and functional effects of Na<sub>2</sub>EDTA on the outflow routes for aqueous humor in monkeys. *Exp. Eye Res.* 44, 171–190.
- Hedbys, B.O., Mishima, S., 1962. Flow of water in corneal stroma. *Exp. Eye Res.* 1, 262–275.
- Heimark, R.L., Kaochar, S., et al., 2002. Human Schlemm's canal cells express the endothelial adherens proteins, VE-cadherin and PECAM-1. *Curr. Eye Res.* 25, 299–308.
- Holmberg, A., 1959. The fine structure of the inner wall of Schlemm's canal. *Arch. Ophthalmol.* 62, 956–958.
- Holmberg, A., 1965. Schlemm's canal and the trabecular meshwork. An electron microscopic study of the normal structure in man and monkey (*Cercopithecus ethiops*). *Doc. Ophthalmol.* 19, 339–375.
- Huggert, A., 1955. Pore size in the filtration angle of the eye. *Acta Ophthalmol.* 33, 271–284.
- Huggert, A., Holmberg, A., et al., 1955. Further studies concerning the filtration angle of the eye. *Acta Ophthalmol.* 33, 429–436.
- Johnson, M., Erickson, K., 2000. Mechanisms and routes of aqueous humor drainage. In: Albert, D.M., Jakobiec, F.A. (Eds.), *Principles and Practice of Ophthalmology*, vol. 4. Saunders, Philadelphia, pp. 2577–2595 (Chapter 193B, Glaucoma).
- Johnson, M., Kamm, R.D., 1983. The role of Schlemm's canal in aqueous outflow from the human eye. *Invest. Ophthalmol. Vis. Sci.* 24, 320–325.
- Johnson, M., Johnson, D.H., et al., 1990. The filtration characteristics of the aqueous outflow system. *Exp. Eye Res.* 50, 407–418.
- Johnson, M., Shapiro, A., et al., 1992. Modulation of outflow resistance by the pores of the inner wall endothelium. *Invest. Ophthalmol. Vis. Sci.* 33, 1670–1675.
- Johnson, M., Chen, D., et al., 2002. Glaucomatous eyes have a reduced pore density in the inner wall endothelium of Schlemm's canal. *Invest. Ophthalmol. Vis. Sci.* 43, 2950–2955.
- Johnstone, M.A., 1979. Pressure-dependent changes in nuclei and the process orgins of the endothelial cells lining Schlemm's canal. *Invest. Ophthalmol. Vis. Sci.* 18, 44–51.
- Johnstone, M.A., Grant, W.M., 1973. Pressure dependent changes in the structures of the aqueous outflow system of human and monkey eyes. *Am. J. Ophthalmol.* 75, 365.
- Kaida, M., Cao, F., et al., 2000. Time at confluence for human RPE cells: effects on the adherens junction and in vitro wound closure. *Invest. Ophthalmol. Vis. Sci.* 41, 3215–3224.
- Kamm, R.D., Palaszewski, B.A., et al., 1983. Calculation of flow resistance in the juxtacanalicular meshwork. ARVO abstracts. *Invest. Ophthalmol. Vis. Sci.* 24, 135.
- Karg, S.J., Garron, L.K., et al., 1959. Perfusion of human eyes with latex microspheres. *Arch. Ophthalmol.* 61, 68–71.
- Klyce, S.D., Russell, S.R., 1979. Numerical solution of coupled transport equations applied to corneal hydration dynamics. *J. Physiol.* 292, 107–134.
- Kubosawa, J., Kondo, Y., 1994. Quick-freeze, deep-etch studies of renal basement membranes. *Microsc. Res. Tech.* 28, 2–12.
- Leber, T., 1873. Studien über den Flüssigkeitswechsel im auge. *Albrecht Graefes Arch. Ophthalmol.* 19, 87–106.
- Lee, W.R., Grierson, L., 1975. Pressure effects on the endothelium of the trabecular wall of Schlemm's canal: a study by scanning electron microscopy. *Graefes Arch. Clin. Exp. Ophthalmol.* 196, 255–265.
- Levick, J.R., 1987. Flow through interstitium and other fibrous matrices. *Q. J. Exp. Physiol.* 72, 409–437.
- Levick, J.R., Smaje, L.H., 1987. An analysis of the permeability of a fenestra. *Microvasc. Res.* 33, 233–256.
- Levick, J.R., Price, F.M., et al., 1996. Synovial matrix–synovial fluid system of joints, *Extracellular Matrix*, vol. I. Harwood Academic Publishers, W.D. Comper, Amsterdam, pp. 328–377.
- Lütjen-Drecoll, E., Futa, R., et al., 1981. Ultrahistochemical studies on tangential sections of trabecular meshwork in normal and glaucomatous eyes. *Invest. Ophthalmol. Vis. Sci.* 21, 563–573.
- Lütjen-Drecoll, E., Rittig, M., et al., 1989. Immunomicroscopical study of type VI collagen in the trabecular meshwork of normal and glaucomatous eyes. *Exp. Eye Res.* 48, 139–147.
- Maepea, O., Bill, A., 1989. The pressures in the episcleral veins, Schlemm's canal and the trabecular meshwork in monkeys: effects of changes in intraocular pressure. *Exp. Eye Res.* 49, 645–663.
- Maepea, O., Bill, A., 1992. Pressures in the juxtacanalicular tissue and Schlemm's canal in monkeys. *Exp. Eye Res.* 54, 879–883.
- Marshall, G.E., Konstas, A.G., et al., 1990. Immunogold localization of type IV collagen and laminin in the aging human outflow system. *Ophthalmology* 98, 692–700.
- Marshall, G.E., Konstas, A.G., et al., 1991. Immunogold ultrastructural localization of collagen in the aged human outflow system. *Ophthalmology* 98, 692–700.
- Marshall, J., Hussain, A.A., et al., 1998. Aging and Bruch's membrane. In: Marmor, M.F., Wolfensberger, T.J. (Eds.), *The Retinal Pigment Epithelium: Function and Disease*. Oxford University Press, New York, pp. 669–692.
- McEwen, W.K., 1958. Application of Poiseuille's law to aqueous outflow. *Arch. Ophthalmol.* 60, 290.
- Mecham, R.P., Heuser, J., 1990. Three-dimensional organization of extracellular matrix in elastic cartilage as viewed by quick freeze, deep etch electron microscopy. *Connect. Tissue Res.* 24, 83–93.
- Moses, R.A., 1977. The effect of intraocular pressure on resistance to outflow. *Surv. Ophthalmol.* 22, 88–100.
- Moses, R.A., 1979. Circumferential flow in Schlemm's canal. *Am. J. Ophthalmol.* 88, 585–591.
- Mow, V.C., Holmes, M.H., et al., 1984. Fluid transport and mechanical properties of articular cartilage: a review. *J. Biomech.* 17, 377.
- Murphy, C.G., Johnson, M., et al., 1992. Juxtacanalicular tissue in pigmentary and primary open angle glaucoma. The hydrodynamic role of pigment and other constituents. *Arch. Ophthalmol.* 110, 1779–1785.
- Neal, C.R., Michel, C.C., 1995. Transcellular gaps in microvascular walls of frogs and rat when permeability is increased by perfusion with the ionophore A23187. *J. Physiol.* 488.2, 427–437.
- Neal, C.R., Michel, C.C., 1996. Openings in frog microvascular endothelium induced by high intravascular pressures. *J. Physiol.* 492, 39–52.
- Nesterov, A.P., 1970. Role of blockade of Schlemm's canal in pathogenesis of primary open angle glaucoma. *Am. J. Ophthalmol.* 70, 691–696.
- Overby, D., Ruberti, J., et al., 2001. Specific hydraulic conductivity of corneal stroma as seen by quick-freeze/deep-etch. *J. Biomech. Eng.* 123, 154–161.
- Overby, D., Gong, H., et al., 2002. The mechanism of increasing outflow facility during washout in the bovine eye. *Invest. Ophthalmol. Vis. Sci.* 43, 3455–3464.
- Palade, G.E., Simionescu, M., et al., 1979. Structural aspects of the permeability of the microvascular endothelium. *Acta Physiol. Scand.* 463, 11–32.
- Pappenheimer, J., Renkin, E., et al., 1951. Filtration, diffusion and molecular sieving through peripheral capillary membranes: a contribution to the pore theory of capillary permeability. *Am. J. Physiol.* 167, 13–46.
- Penfold, P.L., Wen, L., et al., 2000. Triamcinolone acetonide modulates permeability and intercellular adhesion molecule-1 (ICAM-1) expression of the ECV304 cell line: implications for macular degeneration. *Clin. Exp. Immunol.* 121, 458–465.
- Perkins, T.W., Alvarado, J.A., et al., 1988. Trabecular meshwork cells grown on filters. Conductivity and cytochalasin effects. *Invest. Ophthalmol. Vis. Sci.* 29, 1836–1846.
- Persson, B.E., Spring, K.R., 1982. Gallbladder epithelial cell hydraulic water permeability and volume regulation. *J. Gen. Physiol.* 79, 481–505.
- Peterson, W.S., Jocsos, V.L., 1974. Hyaluronidase effects on aqueous outflow resistance. *Am. J. Ophthalmol.* 77, 573–577.
- Preston, G.M., Carroll, T.P., et al., 1992. Appearance of water channels in *Xenopus* oocytes expressing red cell CHIP28 protein. *Science* 256, 385–387.
- Rao, P.V., Deng, P.F., et al., 2001. Modulation of aqueous humor outflow facility by the Rho kinase-specific inhibitor Y-27632. *Invest. Ophthalmol. Vis. Sci.* 42, 1029–1037.

- Raviola, G., Raviola, E., 1981. Paracellular route of aqueous outflow in the trabecular meshwork and canal of Schlemm. *Invest. Ophthalmol. Vis. Sci.* 21, 52–72.
- Renkin, E.M., 1977. Multiple pathways of capillary permeability. *Circ. Res.* 41, 735–743.
- Robertson, G.B., Walton, H.A., 1989. Glomerular basement membrane as a compressible ultrafilter. *Microvasc. Res.* 38, 36–48.
- Rohen, J.W., Rentsch, T.J., 1968. Über den Bau des Schlemmschen Kanals und seiner Abflussweg beim Menschen. *Graefes Arch. Clin. Exp. Ophthalmol.* 176, 309–329.
- Rosenquist, R., Epstein, D., et al., 1989. Outflow resistance of enucleated human eyes at two different perfusion pressures and different extents of trabeculotomy. *Curr. Eye Res.* 8, 1233–1240.
- Savla, U., Neal, C.R., et al., 2002. Openings in frog microvascular endothelium at different rates of increase in pressure and at different temperatures. *J. Physiol.* 539, 285–293.
- Seidel, E., 1921. Weitere experimentelle Untersuchungen über die Quelle und den Verlauf der intraokularen Saftströmung. IX Mitteilung. Über den Abfluss des Kammerwassers aus der vorderen Augenkammer. *Graefes Arch. Clin. Exp. Ophthalmol.* 104, 357–402.
- Seiler, T., Wollensak, J., 1985. The resistance of the trabecular meshwork to aqueous humor outflow. *Graefes Arch. Clin. Exp. Ophthalmol.* 223, 88–91.
- Sill, H.W., Cecil, B., et al., 1992. Albumin permeability and electrical resistance as means of assessing endothelial monolayer integrity in vitro. *J. Tissue Cult. Methods* 14, 253–258.
- Simionescu, M., Simionescu, N., et al., 1978. Open junctions in the endothelium of the postcapillary venules of the diaphragm. *J. Cell. Biol.* 79, 27–44.
- Sit, A.J., Coloma, F.M., et al., 1997. Factors affecting the pores of the inner wall endothelium of Schlemm's canal. *Invest. Ophthalmol. Vis. Sci.* 38, 1517–1525.
- Solomon, A.K., Chasan, B., et al., 1983. The aqueous pore in the red cell membrane: band 3 as a channel for anions, cations, nonelectrolytes, and water. *Ann. NY Acad. Sci.* 414, 97–124.
- Speakman, J.S., 1959. Aqueous outflow channels in the trabecular meshwork in man. *Br. J. Ophthalmol.* 43, 129.
- Stamer, W.D., Seftor, R.E., et al., 1995. Cultured human trabecular meshwork cells express aquaporin-1 water channels. *Curr. Eye Res.* 14, 1095–1100.
- Starita, C., Hussain, A., et al., 1996. Hydrodynamics of ageing Bruch's membrane: implications for macular disease. *Exp. Eye Res.* 62, 565–572.
- Starita, C., Hussain, A.A., et al., 1997. Localization of the major site of resistance to fluid transport in Bruch's membrane. *Invest. Ophthalmol. Vis. Sci.* 38, 762–767.
- Ten Hulzen, R.D., Johnson, D.H., 1996. Effect of fixation pressure on juxtacanalicular tissue and Schlemm's canal. *Invest. Ophthalmol. Vis. Sci.* 37, 114–124.
- Tervo, K., Päällysaho, T., et al., 1995. Integrins in human anterior chamber angle. *Graefes Arch. Clin. Exp. Ophthalmol.* 233, 291–292.
- Timbs, M.M., Spring, K.R., 1996. Hydraulic properties of MDCK cell epithelium. *J. Membr. Biol.* 153, 1–11.
- Tripathi, R., 1974a. Tracing the bulk outflow route of cerebrospinal fluid by transmission and scanning electron microscopy. *Brain Res.* 80, 503–506.
- Tripathi, R.C., 1974b. Comparative physiology and anatomy of the aqueous outflow pathway. In: Davson, H., Graham, L.T., et al. (Eds.), *The Eye Comparative Physiology*, vol. 5. Academic Press, New York, NY, pp. 163–356 (Chapter 3).
- Tripathi, R.C., 1977. The functional morphology of the outflow systems of ocular and cerebrospinal fluids. *Exp. Eye Res.* 25, 65–116.
- Tsuboi, S., 1987. Measurement of the volume flow and hydraulic conductivity across the isolated dog retinal pigment epithelium. *Invest. Ophthalmol. Vis. Sci.* 28, 1776–1782.
- Underwood, J.L., Murphy, C.G., et al., 1999. Glucocorticoids regulate transendothelial fluid flow resistance and formation of intercellular junctions. *Am. J. Physiol.* 277, C330–C342.
- Van Buskirk, E.M., 1976. Changes in the facility of aqueous outflow induced by lens depression and intraocular pressure in excised human eyes. *Am. J. Ophthalmol.* 82, 736–740.
- Van Buskirk, E.M., 1977. Trabeculotomy in the immature, enucleated human eye. *Invest. Ophthalmol. Vis. Sci.* 16, 63–66.
- Van Buskirk, E.M., Grant, W.M., 1973. Lens depression and aqueous outflow in enucleated primate eyes. *Am. J. Ophthalmol.* 72, 632–640.
- Van Buskirk, E.M., Pond, V., et al., 1984. Argon laser trabeculoplasty. *Studies of mechanism of action. Ophthalmology* 91, 1005–1010.
- Vargas, C.B., Vargas, F.F., et al., 1979. Hydraulic conductivity of the endothelial and outer layers of rabbit aorta. *Am. J. Physiol.* 236, H53–H60.
- Welling, L., Welling, D., 1978. Physical properties of isolated perfused basement membranes from rabbit loop of Henle. *Am. J. Physiol.* 234, F54–F58.
- Wise, J.B., Witter, S.L., 1979. Argon laser therapy for open-angle glaucoma. A pilot study. *Arch. Ophthalmol.* 97, 319–322.
- Yaccino, J.A., Chang, Y.S., et al., 1997. Physiological transport properties of cultured retinal microvascular endothelial cell monolayers. *Curr. Eye Res.* 16, 761–768.
- Ye, W., Gong, H., et al., 1997. Interendothelial junctions in normal human Schlemm's canal respond to changes in pressure. *Invest. Ophthalmol. Vis. Sci.* 38, 2460–2468.